# Electrochemical Sensor for Rapid Detection of Triclosan Using a Multiwall Carbon Nanotube Film

JINQUAN YANG,[†] PENG WANG,[‡] XIAOJUN ZHANG,[†,§] AND KANGBING WU*,[†]

[†]Department of Chemistry, Huazhong University of Science and Technology, Wuhan 430074, People's Republic of China, [‡]Hubei Entry−Exit Inspection and Quarantine Bureau of People's Republic of China, Wuhan 430022, People's Republic of China, and [§]SINOPEC Changling Company, Yueyang 414012, People's Republic of China

It is of great importance to develop a rapid analytical method for triclosan because it has been widely added in household products and can form highly toxic dioxin-type derivatives. Herein, an electrochemical sensor based on a multiwall carbon nanotube (MWCNT) film was developed for the rapid detection of triclosan. The electrochemical responses of triclosan were examined, given that its oxidation is irreversible and involves one electron. At the MWCNT film, the oxidation signals of triclosan remarkably increase, suggesting that the MWCNT film exhibits a considerable enhancement effect with triclosan. The analytical parameters, such as pH value, amount of MWCNT suspension, and accumulation time, were optimized. The linear range is from 50 $\mu$g L$^{-1}$ to 1.75 mg L$^{-1}$, and the limit of detection is 16.5 $\mu$g L$^{-1}$ (about 57 nM). Finally, the new method was successfully employed to detect triclosan in different toothpaste samples, which was testified using high-performance liquid chromatography (HPLC).

KEYWORDS: Triclosan; electrochemical sensor; rapid determination; carbon nanotube

## INTRODUCTION

Triclosan (5-chloro-2-(2,4-dichlorophenoxy)phenol, **Figure 1**) is an antimicrobial widely used in household products, such as toothpastes, soaps, fabrics, and plastics. However, recent studies show that triclosan can form highly toxic dioxin-type derivatives, such as chlorophenols and chloroform (*1−3*). Therefore, it is crucial to develop a rapid, sensitive, and convenient analytical method for triclosan.

From the molecular structure, it is very clear that triclosan contains phenolic hydroxyl, which is electrochemically active and can be oxidized under proper conditions. Therefore, various electrochemical methods have been reported for the determination of triclosan. For example, the electrochemical behavior of triclosan at the screen-printed carbon electrode (SPCE) was investigated, and an electrochemical method with a limit of detection (LOD) of 1.2 $\mu$M was then developed (*4*). On the basis of the adsorption of triclosan on the hanging mercury drop electrode, another electrochemical method was reported (*5*). Although the LOD is as low as 6.6 nM, a toxic mercury electrode is used. Otherwise, a carbon nanoparticles/ poly(diallyldimethylammonium chloride) composite film with a LOD of 0.5 $\mu$M (*6*), a cellulose-PDDAC film with a LOD of 1 $\mu$M (*7*), a tosyl-functionalized carbon nanoparticles with a LOD of 10 $\mu$M (*8*), and an electropolymerized molecularly imprinted polymer with a LOD of 80 nM (*9*) were also reported for the electrochemical determination of triclosan. However, to the best of our knowledge, electrochemical detection of triclosan using a carbon nanotube (CNT) film has not been published.

Owing to the unique properties, the CNT film has obtained much attention and been widely used in various fields, such as batteries (*10*), fuel cells (*11*), supercapacitors (*12*), adsorption (*13*), catalysis (*14*), and electrochemical detection (*15−18*). The main objective of this work is to develop a novel electroanalytical method for triclosan based on the distinctive properties of CNT film. To accomplish this, the insoluble multiwall carbon nanotube (MWCNT) solid was first dispersed into water through successive ultrasonication to give a stable and homogeneous MWCNT suspension. After that, the MWCNT film was constructed on the surface of a glassy carbon electrode (GCE) via the method of dip-coating and evaporating. The electrochemical behaviors of triclosan at MWCNT film were examined, indicating that the oxidation of triclosan is irreversible and involves one electron transfer. In comparison to the unmodified GCE, the MWCNT film-modified GCE (MWCNT/GCE) remarkably enhances the oxidation signals of triclosan, which attributed to its large surface area and high accumulation efficiency. Therefore, the MWCNT film must greatly improve the sensitivity of electrochemical detection of triclosan.

## EXPERIMENTAL SECTION

**Reagents.** All of the chemicals were of analytical grade and used directly. MWCNT (purity > 95%) was purchased from Shenzhen Nanotech Port Co., Ltd., China. Dihexadecyl hydrogen phosphate (DHP) was obtained from Fluka (Buchs, Switzerland). Triclosan was purchased from Sigma and dissolved into 0.1 M NaOH to prepare 0.5 g L$^{-1}$ standard solution. The water used was redistilled.

**Instruments.** All of the electrochemical measurements were performed using a CHI 610B electrochemical workstation (Shanghai Chenhua Instrument Co., Ltd., China) in a conventional three-electrode system.

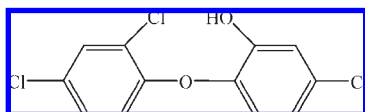*To whom correspondence should be addressed. E-mail: kbwu@ mail.hust.edu.cn.

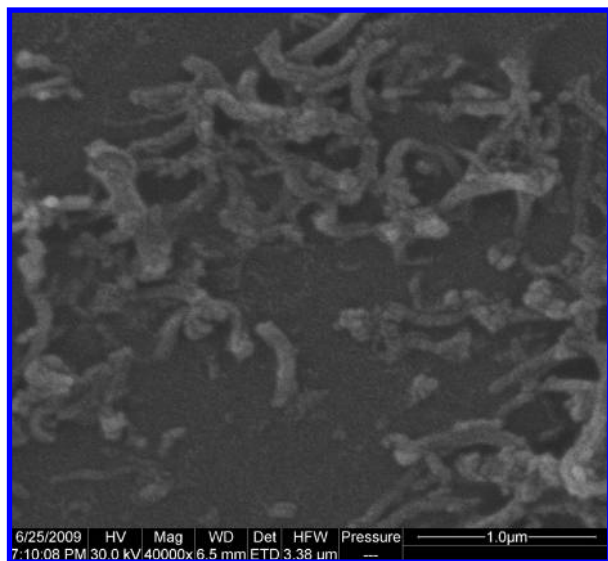**Figure 1.** Molecular structure of triclosan.



**Figure 2.** SEM image of the MWCNT film on the GCE surface.

The working electrode is MWCNT/GCE; the reference electrode is saturated calomel electrode (SCE); and the auxiliary electrode is platinum wire.

Scanning electron microscopy (SEM) was performed with a Sirion 200 microscope (FEI Company, Netherlands).

High-performance liquid chromatographic detection was carried out with an Agilent 1100, coupled with a UV−vis detector. The C18 analytical column (4.6 mm × 150 mm × 5 $\mu$m) was used. The mobile phase was methanol/H$_2$O (90:10, v/v), filtered through a 0.2 $\mu$m Millipore filter prior to use. The flow rate was 1 mL min$^{-1}$, and the sample injection volume was 20 $\mu$L. The detection was performed at a wavelength of 280 nm.

**Preparation of MWCNT/GCE.** Before modification, the GCE surface (Gaoss Union Co., Ltd., China) was polished with 0.05 $\mu$m alumina slurry and then sonicated in redistilled water to give a clean surface. The MWCNT suspension (1 mg mL$^{-1}$) was prepared by 40 min ultrasonic dispersion of MWCNT and DHP into water. Finally, the treated GCE surface was coated with a 5 $\mu$L MWCNT suspension and allowed to evaporate water under an infrared lamp. The surface morphology of MWCNT/GCE was characterized using SEM, which was shown in **Figure 2**. In the SEM image, uniform and pure CNTs were observed on the GCE surface and the average diameter is about 20 nm.

**Sample Preparation.** Different toothpaste samples were purchased from a local supermarket and treated according to the Industrial Standard of Light Industry, People's Republic of China (QB/T 2969-2008). The sample (about 0.5 g) was exactly weighed and then ultrasonicated in 10 mL of 70% ethanol (v/v) for 40 min. After that, the filtrate was collected using 0.45 $\mu$m membrane and diluted to 10.0 mL for further analysis.

**Analytical Procedure.** Unless otherwise stated, pH 7.0 phosphate buffer (0.1 mol L$^{-1}$) was used as the supporting electrolyte for triclosan. After 4 min of accumulation, the differential pulse voltammetry (DPV) curves from 0.10 to 0.80 V were recorded and the oxidation peak current at 0.57 V was measured for triclosan. The pulse amplitude is 50 mV; the pulse width is 40 ms; and the scan rate is 40 mV s$^{-1}$.

## RESULTS AND DISCUSSION

**Electrochemical Behaviors of Triclosan.** The electrochemical behaviors of triclosan at MWCNT/GCE were examined using cyclic voltammetry (CV). **Figure 3** shows the successive CVs of
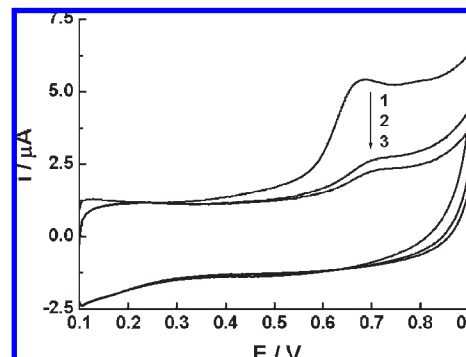


**Figure 3.** CVs of 5 mg L$^{-1}$ triclosan in pH 7.0 phosphate buffer on MWCNT/GCE. Scan rate = 100 mV s$^{-1}$.
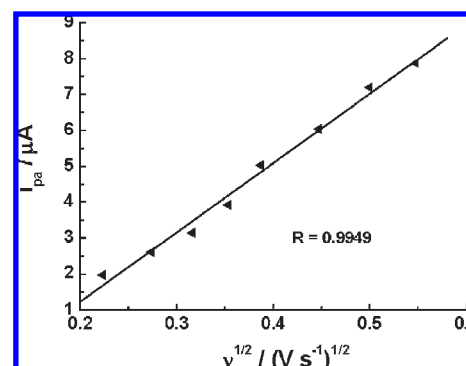


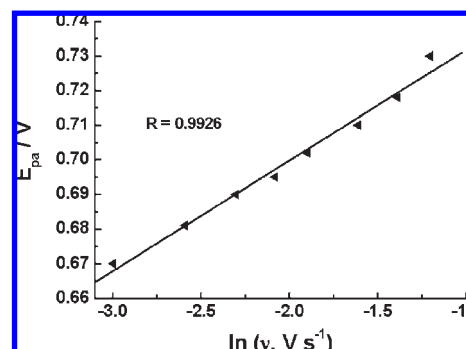**Figure 4.** Plot of $i_{pa}$ versus $\nu^{1/2}$. Other conditions are the same as in **Figure 3**.



**Figure 5.** Relationship between $E_{pa}$ and ln($\nu$). Other conditions are the same as in **Figure 3**.

5 mg L$^{-1}$ triclosan at MWCNT/GCE in pH 7.0 phosphate buffer. During the anodic sweep from 0.10 to 0.90 V, an oxidation peak at 0.69 V is observed. On the reverse scan from 0.90 to 0.10 V, no reduction peak appears, indicating that the oxidation of triclosan is irreversible. During the following cyclic sweeps, the oxidation peak current remarkably decreases, maybe caused by the fact that the oxidative product of triclosan adsorbs at the MWCNT film surface. On the other hand, the CV responses of MWCNT/GCE in pH 7.0 phosphate buffer without triclosan were also studied. The CV curve is smooth, and no peaks are observed, suggesting that the oxidation peak at 0.69 V corresponds to triclosan.

The electrochemical responses of triclosan under different scan rates ($\nu$) were studied using CV. When gradually increasing $\nu$ from 0.05 to 0.30 V s$^{-1}$, only an oxidation peak is observed at MWCNT/GCE and the oxidation peak current ($i_{pa}$) increases linearly with the square root of $\nu$, as shown in **Figure 4**. The linear relationship between $i_{pa}$ and $\nu^{1/2}$ suggests that the oxidation of
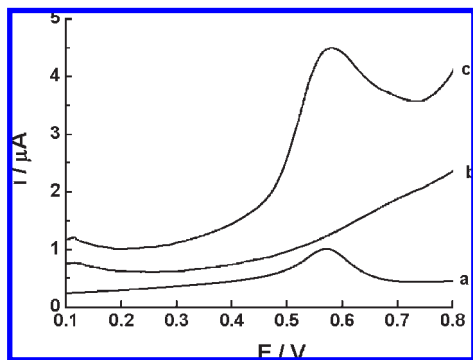
**Figure 6.** DPV curves of 0.5 mg L$^{-1}$ triclosan in pH 7.0 phosphate buffer at (a) GCE and (c) MWCNT/GCE. (b) Blank DPV curve of MWCNT/GCE. Pulse amplitude, 50 mV; pulse width, 40 ms; scan rate, 40 mV s$^{-1}$; accumulation time, 4 min.



**Figure 7.** Effect of the pH value on the oxidation peak current of 0.5 mg L$^{-1}$ triclosan at MWCNT/GCE. Other conditions are the same as in **Figure 6**.



**Figure 8.** Dependence of the oxidation peak current of 0.5 mg L$^{-1}$ triclosan on the amount of MWCNT suspension. Other conditions are the same as in **Figure 6**.

triclosan is controlled by diffusion. In addition, the oxidation peak potential ($E_{pa}$) of triclosan gradually shifts to more positive potentials when improving $v$, also revealing that the oxidation of triclosan is irreversible. **Figure 5** demonstrates the relationship between $E_{pa}$ and $v$. It was found that the $E_{pa}$ is proportional to $\ln(v)$, obeying the following equation:

$$E_{pa}/V = 0.7637 + 0.03199 \ln(v/Vs^{-1})$$

For an irreversible and diffusion-controlled oxidation process, the $E_{pa}$ is defined by the following equation:

$$E_{pa} = E^{o\prime} + \frac{RT}{\alpha nF}\left[0.780 + \ln\left(\frac{D_R^{1/2}}{k^o}\right) + \ln\left(\frac{\alpha Fv}{RT}\right)^{1/2}\right]$$

$$= K + \frac{RT}{2\alpha nF}\ln(v)$$

where $E^{o\prime}$ is the formal potential, $\alpha$ is the electron-transfer coefficient, $n$ is the number of transferred electrons, $k^o$ is the standard heterogeneous rate constant, and $D_R$ is the diffusion coefficient. Other symbols have their usual significance. Therefore, the value of $\alpha n$ can be easily obtained from the slope of $E_{pa}$ versus $\ln(v)$. Herein, the $\alpha n$ is calculated to be 0.40 for the oxidation of triclosan. Given $0.3 < \alpha < 0.7$, we conclude that $n = 1$ and $\alpha = 0.40$. Thus, the oxidation of triclosan is a single-electron-transfer process, which is in good agreement with the other published work (*4*).

**DPV Responses of a Low Concentration of Triclosan.** To develop an analytical method for trace levels of triclosan and to elucidate the distinctive properties of MWCNT, the electrochemical responses of a low concentration of triclosan at GCE and MWCNT/GCE were studied using DPV. **Figure 6** shows the DPV curves of 0.5 mg L$^{-1}$ triclosan in pH 7.0 phosphate buffer. At the unmodified GCE (curve a), an oxidation peak at 0.57 V is observed during the anodic sweep from 0.10 to 0.80 V. When using MWCNT/GCE (curve c), the oxidation peak of triclosan greatly increases, suggesting that MWCNT film is more active to the oxidation of triclosan. As well-known, the MWCNT film possesses a large surface area, high sorption capacity, and numerous active sites; therefore, the MWCNT/GCE exhibits much higher accumulation efficiency to triclosan and remarkably increases its oxidation peak current. Otherwise, the DPV curve of MWCNT/GCE in pH 7.0 buffer without triclosan was also given in curve b for a better understanding. The blank curve is smooth, and no oxidation peak appears, revealing that the oxidation peak in curve c is attributed to triclosan. From **Figure 6**, a conclusion
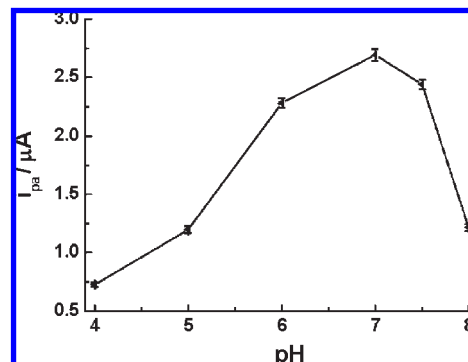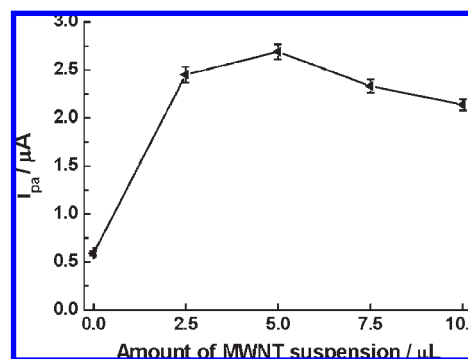
can be made that the sensitivity of detection of triclosan will be greatly improved when using MWCNT film.

**Detection of Triclosan. Figure 7** demonstrates the influence of the pH value on the oxidation peak current of triclosan at MWCNT/GCE. When the pH value is increased from 4.0 to 7.0, the oxidation peak current of triclosan gradually increases. Further when the pH value is increased from 7.0 to 8.0, the peak current gradually decreases. Thus, pH 7.0 phosphate buffer was employed for the detection of triclosan because the oxidation signal is more sensitive.

**Figure 8** illustrates the effect of the amount of MWCNT suspension on the oxidation peak current of triclosan. When the volume of MWCNT suspension is gradually improved from 0 to 5 $\mu$L, the oxidation peak current remarkably increases. When the volume of MWCNT suspension is increased, the surface amount of MWCNT also increases, resulting in a larger surface area and higher accumulation efficiency to triclosan. As a result, the oxidation peak current of triclosan notably increases. However, the oxidation peak current of triclosan gradually decreases with further increasing of the volume from 5 to 10 $\mu$L. This may be due to the fact that DHP lowers the electric conductivity and blocks the electron transfer of triclosan. Considering the oxidation signal and the time for evaporating water, 5 $\mu$L of MWCNT suspension was used to modify the GCE surface.

The effect of the accumulation time on the detection of triclosan was also examined using DPV. **Figure 9** shows the change of the oxidation peak current of triclosan as a function of the accumulation time. When the accumulation time is extended from 0 to 4 min, the oxidation peak current of triclosan remarkably increases, suggesting that accumulation improves the determining sensitivity. When the accumulation time is further

**9406** *J. Agric. Food Chem.,* Vol. 57, No. 20, 2009

Yang et al.
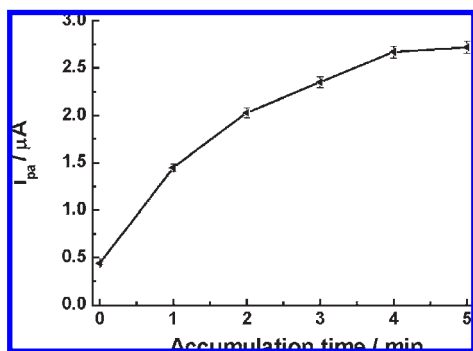


**Figure 9.** Influence of the accumulation time on the oxidation peak current of 0.5 mg L$^{-1}$ triclosan at MWCNT/GCE. Other conditions are the same as in **Figure 6**.

**Table 1.** Detection of Triclosan in Toothpaste Samples

| samples | by HPLC (mg g$^{-1}$) | by this method (mg g$^{-1}$) | RSD (%) | added (mg g$^{-1}$) | found (mg g$^{-1}$) | recovery (%) |
|---|---|---|---|---|---|---|
| Colgate A | 1.95 | 2.42 | 5.9 | 0.992 | 1.043 | 105.1 |
| Colgate B | not found | not found | | 0.924 | 0.961 | 104.0 |
| Liubi Zhi | 0.356 | 0.431 | 4.2 | 0.852 | 0.830 | 97.4 |
| Darlie | not found | not found | | 0.978 | 1.05 | 107.4 |

improved from 4 to 5 min, the oxidation peak current increases slightly and a platform appears, revealing that the amount of triclosan at the MWCNT/GCE surface tends to be a limiting value. Considering sensitivity and analysis time, the accumulation time was selected as 4 min.

**Precision, Linear Range, and LOD.** The MWCNT/GCE was used for single measurement because the surface sorption is strong. The precision between multiple MWCNT/GCEs was estimated by determining the response of 0.5 mg L$^{-1}$ triclosan. The relative standard deviation (RSD) is 4.4% for 10 MWCNT/GCEs, indicative of acceptable fabrication reproducibility and good determining precision.

The linear range for triclosan was examined using DPV after 4 min of accumulation. It was found that the oxidation peak current of triclosan ($i_{pa}$, μA) is proportional to its concentration ($C$, mg L$^{-1}$) over the range from 50 μg L$^{-1}$ to 1.75 mg L$^{-1}$, obeying the following equation: $i_{pa} = 0.117 + 5.146C$ ($R = 0.996$). In addition, the LOD after 4 min of accumulation was evaluated to be 16.5 μg L$^{-1}$ (about 57 nM) based on a signal/noise ratio of 3.

**Analytical Application.** To assess the performance of this method in real sample analysis, it was used to determine triclosan in several toothpaste samples. Each sample solution undergoes three parallel detections, and the RSD is below 6%, suggesting that the results obtained by MWCNT/GCE are acceptable. The content of triclosan was determined by the method of standard addition, and the results are listed in **Table 1**. To testify the accuracy of this method, the content of triclosan was also analyzed by high-performance liquid chromatography (HPLC). The results obtained by HPLC and MWCNT/GCE are in good agreement, revealing that this method is satisfactory. In addition, a known amount of triclosan standard was spiked in the sample and then analyzed according to the same procedure. The value of recovery is in the range from 97.4 to 107.4%, also indicating that this method is accurate and feasible.

**CONCLUSION**

The electrochemical behaviors of triclosan at the MWCNT film-modified electrode were investigated, and an irreversible

oxidation peak that involved one electron was observed. Owing to the large surface area, high sorption ability, and numerous active sites, the MWCNT film remarkably increases the oxidation signals of triclosan. As a result, a sensitive electrochemical method was developed for triclosan. Otherwise, this method possesses a short analysis time and excellent simplicity in comparison to other methods, such as HPLC. Finally, it was successfully used to detect triclosan in toothpastes, and the accuracy was testified using HPLC.

**LITERATURE CITED**

(1) Latch, D. E.; Packer, J. L.; Arnold, W. A.; McNeil, K. Photochemical conversion of triclosan to 2,8-dichlorodibenzo-*p*-dioxin in aqueous solution. *J. Photochem. Photobiol. A-Chem.* **2003**, *158*, 63–66.

(2) Rule, K. L.; Ebbett, V. R.; Vikesland, P. J. Formation of chloroform and chlorinated organics by free-chlorine-mediated oxidation of triclosan. *Environ. Sci. Technol.* **2005**, *39*, 3176–3185.

(3) Fiss, E. M.; Rule, K. L.; Vikesland, P. J. Formation of chloroform and other chlorinated byproducts by chlorination of triclosan-containing antibacterial products. *Environ. Sci. Technol.* **2007**, *41*, 2387–2394.

(4) Pemberton, R. M.; Hart, J. P. Electrochemical behaviour of triclosan at a screen-printed carbon electrode and its voltammetric determination in toothpaste and mouthrinse products. *Anal. Chim. Acta* **1999**, *390*, 107–115.

(5) Safavi, A.; Maleki, N.; Shahbaazi, H. R. Electrochemical determination of triclosan at a mercury electrode. *Anal. Chim. Acta* **2003**, *494*, 225–233.

(6) Amiri, M.; Shahrokhian, S.; Psillakis, E.; Marken, F. Electrostatic accumulation and determination of triclosan in ultrathin carbon nanoparticle composite film electrodes. *Anal. Chim. Acta* **2007**, *593*, 117–122.

(7) Bonne, M. J.; Edler, K. J.; Buchanan, J. G.; Wolverson, D.; Psillakis, E.; Helton, M.; Thielemans, W.; Marken, F. Thin-film modified electrodes with reconstituted cellulose−PDDAC films for the accumulation and detection of triclosan. *J. Phys. Chem. C* **2008**, *112*, 2660–2666.

(8) Vidal, L.; Chisvert, A.; Canals, A.; Psillakis, E.; Lapkin, A.; Acosta, F.; Edler, K. J.; Holdaway, J. A.; Marken, F. Chemically surface-modified carbon nanoparticle carrier for phenolic pollutants: Extraction and electrochemical determination of benzophenone-3 and triclosan. *Anal. Chim. Acta* **2008**, *616*, 28–35.

(9) Liu, Y.; Song, Q. J.; Wang, L. Development and characterization of an amperometric sensor for triclosan detection based on electro-polymerized molecularly imprinted polymer. *Microchem. J.* **2009**, *91*, 222–226.

(10) Morris, R. S.; Dixon, B. G.; Gennett, T.; Raffaelle, R.; Heben, M. J. High-energy, rechargeable Li-ion battery based on carbon nanotube technology. *J. Power Sources* **2004**, *138*, 277–280.

(11) Michel, M.; Taylor, A.; Sekol, R.; Podsiadlo, P.; Ho, P.; Kotov, N.; Thompson, L. High-performance nanostructured membrane electrode assemblies for fuel cells made by layer-by-layer assembly of carbon nanocolloids. *Adv. Mater.* **2007**, *19*, 3859–3864.

(12) Lee, S. W.; Kim, B. S.; Chen, S.; Horn, Y. S.; Hammond, P. T. Layer-by-layer assembly of all carbon nanotube ultrathin films for electrochemical applications. *J. Am. Chem. Soc.* **2009**, *131*, 671–679.

(13) Lee, C. Y.; Strano, M. S. Amine basicity (p$K_b$) controls the analyte binding energy on single walled carbon nanotube electronic sensor arrays. *J. Am. Chem. Soc.* **2008**, *130*, 1766–1773.

(14) Smajda, R.; Kukovecz, A.; Konya, Z.; Kiricsi, I. Structure and gas permeability of multi-wall carbon nanotube buckypapers. *Carbon* **2007**, *45*, 1176–184.

(15) Luo, H. X.; Shi, Z. J.; Li, N. Q.; Gu, Z. N.; Zhuang, Q. K. Investigation of the electrochemical and electrocatalytic behavior

Article

*J. Agric. Food Chem.,* Vol. 57, No. 20, 2009    **9407**

of single-wall carbon nanotube film on a glassy carbon electrode. *Anal. Chem.* **2001**, *73*, 915–920.

(16) Wang, F.; Gu, H. W.; Swager, T. M. Carbon nanotube/polythiophene chemiresistive sensors for chemical warfare agents. *J. Am. Chem. Soc*. **2008**, *130*, 5392–5393.

(17) Sun, Y. X.; Fei, J. J.; Hou, J.; Zhang, Q.; Liu, Y. L.; Hu, B. N. Simultaneous determination of dopamine and serotonin on a carbon nanotubes−ionic liquid gel modified glassy carbon electrode. *Microchim. Acta* **2009**, *165*, 373–379.

(18) Zheng, D. Y.; Hu, C. G.; Peng, Y. F.; Hu, S. S. A carbon nanotube/ polyvanillin composite film as an electrocatalyst for the electrochemical oxidation of nitrite and its application as a nitrite sensor. *Electrochim. Acta* **2009**, *54*, 4910–4915.